CHAPTER 9

Nd:YAG Ceramic ThinZag® High-Power Laser Development

Daniel E. Klimek

Principal Research Scientist, Textron Defense Systems, Wilmington, Massachusetts

Alexander Mandl

Principal Research Scientist, Textron Defense Systems, Wilmington, Massachusetts

9.1 Introduction and ThinZag Concept Development

Over the past decade, solid-state lasers have demonstrated remarkable power in scaling. To a large extent, the emergence of solid-state lasers as competitive high-power devices is due to the availability of highly efficient (~60 percent), high-power (> 100 W), low-cost (< $10/W mounted) laser diode bars.

As a laser gain material, Nd:YAG is by far the most commonly used in solid-state lasers, due to a combination of properties that uniquely favor high-power laser performance. The YAG host is a robust, fracture-resistant material with high thermal conductivity. Nd:YAG also has a narrow fluorescent line width, which results in high gain. There has also been a revolutionary development in laser gain material. Cubic structure materials like YAG can now be fabricated as ceramics with optical uniformity that is better than found in YAG crystals (for both dopant uniformity and variations in index of refraction), with scattering loss coefficients comparable to YAG crystals

Report Documentation Page

Form Approved
OMB No. 0704-0188

1. REPORT DATE	2. REPORT TYPE	3. DATES COVERED
2011		

4. TITLE AND SUBTITLE	5a. CONTRACT NUMBER
Nd:YAG Ceramic ThinZag High-Power Laser Development	5b. GRANT NUMBER
	5c. PROGRAM ELEMENT NUMBER
6. AUTHOR(S)	5d. PROJECT NUMBER
	5e. TASK NUMBER
	5f. WORK UNIT NUMBER
7. PERFORMING ORGANIZATION NAME(S) AND ADDRESS(ES) **Textron Defense Systems,Wilmington,MA,01887**	8. PERFORMING ORGANIZATION REPORT NUMBER
9. SPONSORING/MONITORING AGENCY NAME(S) AND ADDRESS(ES)	10. SPONSOR/MONITOR'S ACRONYM(S)
	11. SPONSOR/MONITOR'S REPORT NUMBER(S)

12. DISTRIBUTION/AVAILABILITY STATEMENT
Approved for public release; distribution unlimited.

13. SUPPLEMENTARY NOTES
The original document contains color images.

14. ABSTRACT

15. SUBJECT TERMS

16. SECURITY CLASSIFICATION OF:			17. LIMITATION OF ABSTRACT	18. NUMBER OF PAGES	19a. NAME OF RESPONSIBLE PERSON
a. REPORT	b. ABSTRACT	c. THIS PAGE			
unclassified	**unclassified**	**unclassified**		**18**	

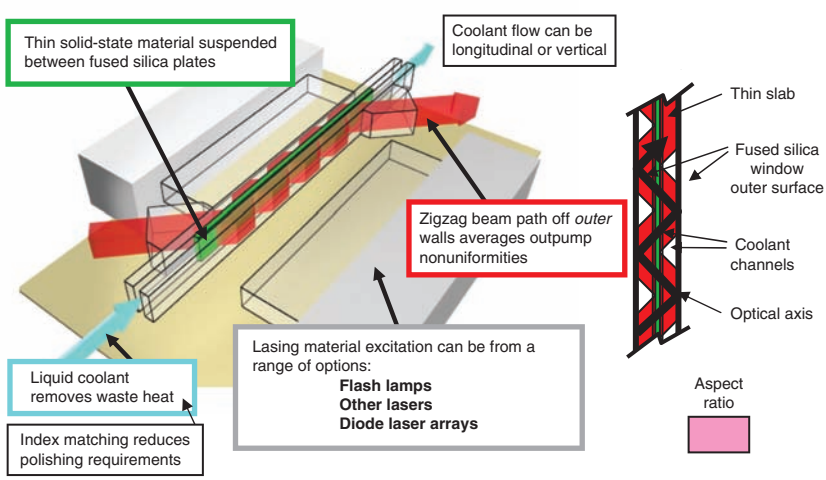

FIGURE 9.1 A schematic drawing of ThinZag configuration, including the key features of the laser and laser beam optical path within the cell.

(< 0.15%/cm). These materials can also be produced in sizes that YAG crystals cannot achieve (e.g., 400×400 mm^2 slabs).[1–3]

The unique properties of Nd:YAG ceramic combined with the ThinZag laser configuration, developed by scientists and engineers at Textron Defense Systems, have allowed scaling of these lasers to more than 16 kW average power from a single laser module. Higher power configurations involve a single-aperture power oscillator configuration consisting of a number of identical modules operating in series.

Figure 9.1 shows a schematic diagram of the ThinZag configuration. With this configuration, improved methods of thermal management for high-power diode-pumped, solid-state slab lasers have been demonstrated. This unique optical arrangement uses thin slabs of solid-state gain material immersed in a flowing cooling fluid and sandwiched between a pair of fused silica windows. The laser flux zigzags through the gain medium in a nontraditional manner—that is, it reflects off the outer surfaces of the fused silica windows rather than off the outer surfaces of the lasing material. The ThinZag configuration allows the use of thin slabs for good thermal control of the laser medium using a near-field beam that has a near-unity aspect ratio that is independent of the laser slab's thickness.

Many features of this design can be varied almost independently to allow optimization of key input parameters to improve performance. This design's orthogonal nature allows for independent variation of parameters such as slab thickness, diode pump intensity, diode pump distribution, thermal cooling rate, number of slabs, and so on.

In addition to the recent development of ceramic Nd:YAG-based devices, tests on a variety of laser gain media have been conducted

over the years at Textron Defense Systems' laser laboratories using the ThinZag configuration. These tests have included flash lamp- and laser-pumped laser arrangements using liquid dye,[4,5] dye-impregnated plastics,[6] and Yb/Er:Glass, Nd:YLF, and Cr:LiSAF crystals.[7–9]

This section describes the progression of ThinZag laser designs from a 1-kW single-slab device (TZ-1) to a 5-kW two-slab device (TZ-2) to a larger-area two-slab nominal 15-kW device (TZ-3). The TZ-3 laser module is the basic building block for achieving higher-power (100-kW) output. Initial tests consist of coupling three TZ-3 modules as a single-aperture power oscillator. The Joint High Power Solid-State Laser (JHPSSL) 100-kW laser consists of six similar modules operating as a single-aperture power oscillator.

9.1.1 TZ-1 Module Development

The first diode-pumped Nd:YAG ThinZag laser (designated TZ-1) was a single-slab design with nominal output ~1 kW. ThinZag lasers at that time used short-pulse lasers or short-pulse flash lamp pumping (~1 μs) as an excitation source. The highest power achieved was about 80 W from a Cr:LiSAF laser, which operated at up to 10 Hz with output up to 8 J/pulse.[4,10,11] The thermal loads for the diode-pumped high-power devices are larger by more than 2 orders of magnitude and call for much greater attention to thermal control of the laser components.

The TZ-1 consisted of a single slab of Nd:YAG (either ceramic or crystal) that is pumped from both sides by high-power 808-nm continuous wave (CW) laser diode arrays. The TZ-1 laser achieved high-power output for extended runs, as shown in Fig. 9.2.

In comparing crystalline and ceramic Nd:YAG samples, it was found that the ceramic samples were generally optically superior to the crystalline samples. Nd:YAG ceramic also displayed better [Nd] uniformity compared to crystal. Typical measurements using a

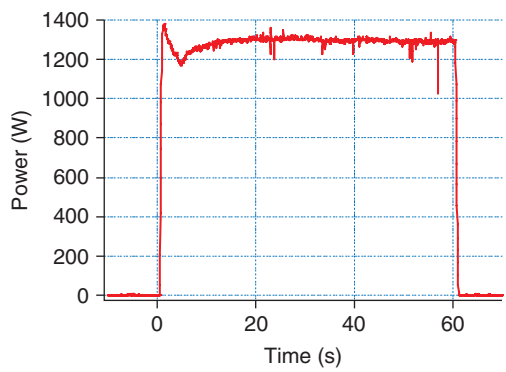

Figure 9.2 Demonstrated steady-state performance of TZ-1 laser using ceramic slab.

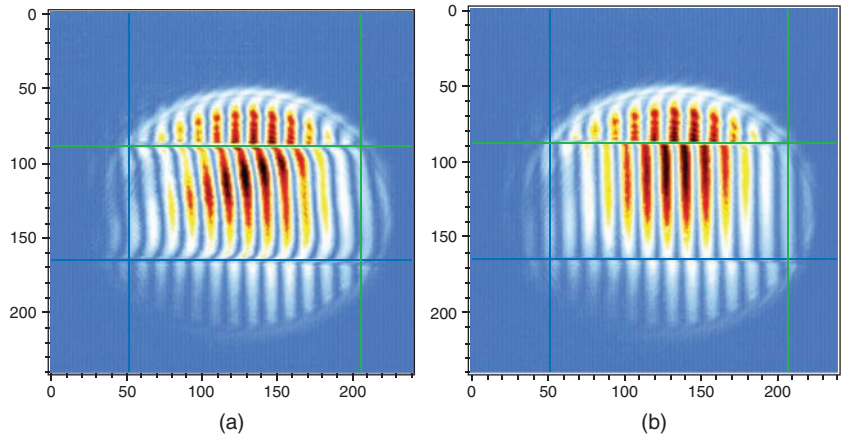

FIGURE 9.3 Double-pass interferometer measurements show that Nd:YAG ceramic slabs are intrinsically more uniform (*b*) than typical crystals (*a*).

two-pass interferometer comparing Nd:YAG crystal with Nd:YAG ceramic slabs are shown in Fig. 9.3. The ceramic slab's index of refraction uniformity was found to be generally superior. Although some crystalline slabs were close in quality to the ceramic slabs, the index variations from one crystal sample to another were significant and unpredictable.

Measurements of laser output using a stable optical cavity verified that ceramic and crystalline slabs of Nd:YAG produced the same output power, within experimental error (~1.2 kW), thus confirming that ceramic gain material was suitable for high-power laser operation. Typical output power measurements are shown in Fig. 9.4.

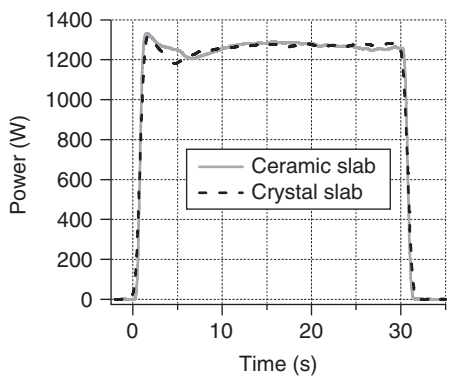

FIGURE 9.4 Comparison of ceramic and crystal slab laser performance.

9.1.2 TZ-2 Module Development

The next scaling path to higher average power was to incorporate a second gain slab into the basic ThinZag laser design. The volume was increased by increasing the slab length by a factor of 1.5, as well as by doubling the number of slabs from one slab to two, for a factor of 3 total increase in excited volume. The pump power was also increased by a factor of 1.5 for an overall deposited pump power increase of 4.5 ($1.5 \times 2 \times 1.5$), thereby projecting an increase in output power to over 5 kW (1.2 kW $\times$ 4.5 = 5.4 kW).

The two-slab ThinZag laser (designated TZ-2) was also pumped from both sides by Nuvonyx diode pump sources, each consisting of 80-W diode bars in series oriented with the fast axis in the horizontal plane. To ensure uniform pumping, the pump light was optically mixed in an optical "scrambler" before reaching the laser module. These scramblers were made of single blocks of fused silica, which acted as a light guide by confining the 808-nm pump radiation using total internal reflection (TIR). Measurements of the pump deposition profile were made using a single scrambler with one of the ThinZag windows. CCD images were taken of the pump light after it passed through the optical scrambler–window combination and impinged onto a Lambertian scattering surface. The measured profiles showed excellent deposition uniformity.

In the center of Fig. 9.5, which shows the TZ-2, the two-slab ThinZag laser head is positioned to show some of the gold-coated metal

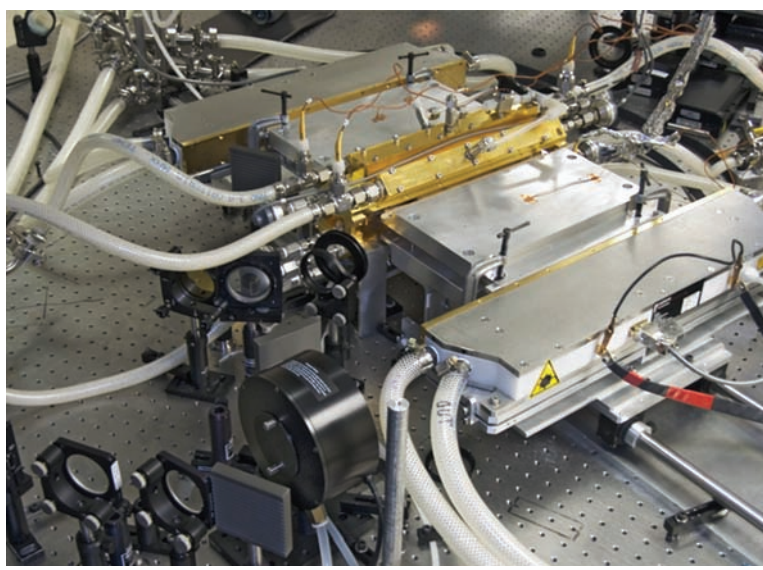

Figure 9.5 TZ-2 laser, showing diode pump source and optical scramblers pumping device from two sides.

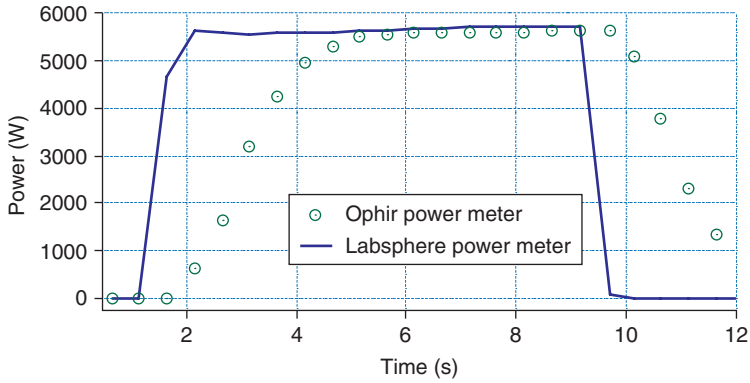

Figure 9.6 Measured laser output power from TZ-2 using a stable optical cavity. Laser output was simultaneously measured by an independently calibrated Ophir power meter (~3-s response time) and an independently calibrated Labsphere power meter (~1-s response time). The diode pump flux incident from each side of the laser slabs was 405 W/cm^2. The calculated optical efficiency (laser output/pump diode output) was 30 percent.

parts. Also shown are the laboratory optical components used for extracting laser light, for making diagnostic measurements, and for recording average power. A trace of the output power versus temporal profile greater than 5 kW is displayed in Fig. 9.6.

The TZ-2 laser was typically operated with a stable optical cavity, using a 4-m radius of curvature primary and a 70 percent reflective feedback flat-output coupler. Figure 9.6 displays two different measurements of laser output: an Ophir power meter, which has a response time of a few seconds, and a Labsphere integrating sphere power meter, which has a response time of about a second. Both instruments are independently calibrated by their manufacturers, and very good agreement was evident. The measured output was about 5.6 kW, which is in good agreement with scaling based on the TZ-1 measurements and the increase in system gain projected from our design changes. These data show an 8-s run with apparent steady-state output. The TZ-2 laser was operated using this stable optical cavity for various operating conditions and runtimes. A 30-s run is shown in Fig. 9.7. No real-time corrections were introduced to handle any thermally induced distortions, such as tilt and focus during this longer run, resulting in a gradual decrease in output with time.

For most applications, lasers must have good beam quality. To evaluate the potential of a ThinZag laser to produce a good-quality optical beam, the laser was placed in one arm of an interferometer, as shown in Fig. 9.8. These measurements were used to provide information on how one might modify the laser module to achieve improved performance. Throughout these tests, the distortions of the

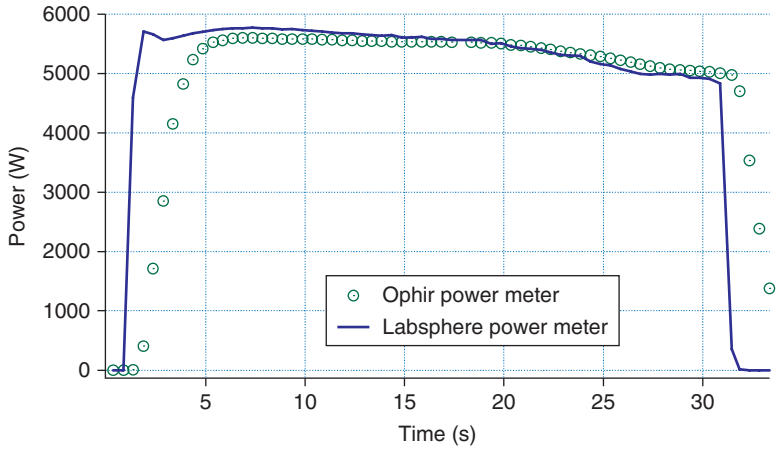

Figure 9.7 A TZ-2 laser output 30-s run using a stable optical cavity has no dynamic correction.

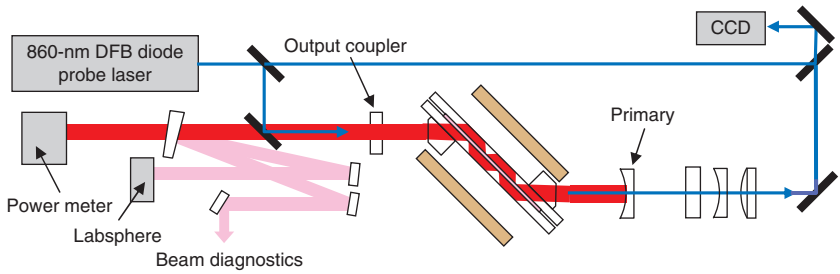

Figure 9.8 Schematic diagram of the setup used to measure interferometric distortions in the laser medium under full diode pump load during laser operation. CCD: charge-coupled device; DFB: distributed feedback.

laser medium were observed to be low order (e.g., focus, astigmatism, tilt, etc.) and slowly varying (time scales of seconds).

The probe laser can be used to measure the medium while the laser operates with a stable optical resonator or, by removing the output coupler, to measure the medium with only the diode pumping. The probe wavelength is in a spectral region in which Nd:YAG has very low absorption. Also shown in Fig. 9.8 are three lenses, which are placed in the optical path to remove low-order static phase errors that result from cell fabrication. These lenses consist of two orthogonal cylindrical lenses and one spherical lens.

Typical interferograms obtained with the TZ-2 laser with and without the resonator mirrors are shown in Fig. 9.9. The top interferogram (Fig. 9.9*a*) is before pumping starts and includes the static

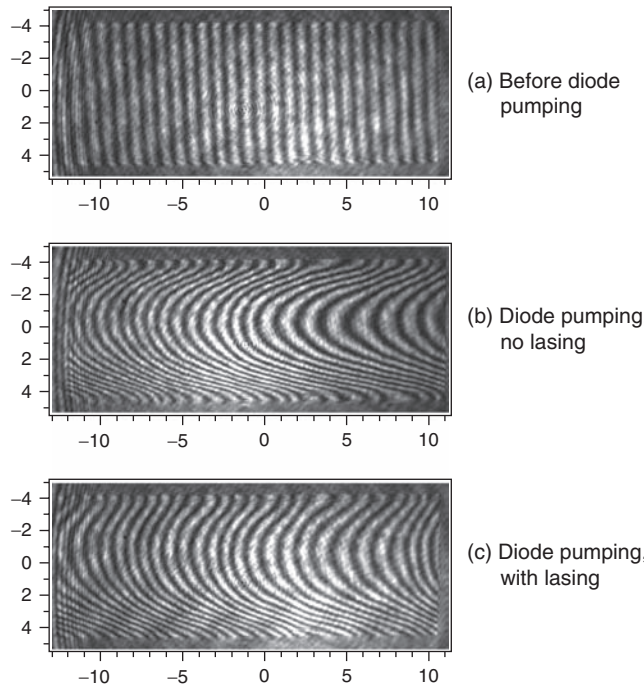

FIGURE 9.9 Measured phase distortion in gain medium (*a*) before diode pumping (with static correction) and during full intensity pumping (*c*) with and (*b*) without lasing.

correctors mentioned above. The data show that only simple distortions of cylinder exist in the medium before pumping and are easily corrected with planocylindrical optics. The next interferogram (Fig. 9.9*b*) shows that about eight waves of primarily vertical cylinder develop as a consequence of the diode pumping. The bottom interferogram (Fig. 9.9*c*), which was taken while the cavity was lasing, shows that the vertical distortion is reduced to about five waves. The distortions shown in Fig. 9.9 develop in about 1 s, with very little change thereafter, with the exception being a slowly growing tilt of about 0.1 waves per second.

Examination of Fig. 9.9*b* and 9.9*c* shows that there are distortions beyond pure cylinder and tilt. Figure 9.10 shows the residual phase-front distortion of the probe beam after both horizontal and vertical cylinders have been mathematically removed. As seen, the variation in the residual is only +1 to –1 waves, most of which is located near the top and bottom edges. As with the cylindrical distortion, there is very little change after about 1 s of operation.

An unstable optical cavity was then set up to perform beam quality measurements on the TZ-2 laser. In order to set up an unstable cavity

Nd:YAG Ceramic ThinZag® High-Power Laser Development

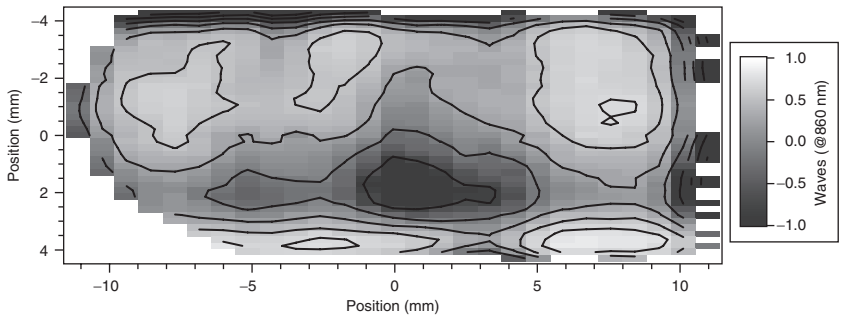

FIGURE 9.10 Residual phase-front distortion after the horizontal and vertical cylinders are removed.

on the TZ-2 module, the optical path was folded to double the gain length. Figure 9.11 is a schematic diagram of the folded TZ-2 cavity. The deformable mirror was added to the cavity to remove the residual distortions depicted in Fig. 9.10.

The TZ-2 laser, when operated with stable optics, has a near-field beam profile of roughly 1×2 cm. With a folded cavity, the beam profile in near field is approximately 1×1 cm. A graded reflectivity mirror (GRM) with a super-Gaussian square profile was designed and subsequently fabricated by INO (National Optics Institute, Quebec, Canada). Laser experiments were performed with this GRM as an output coupler. The measured laser output for this folded cavity was

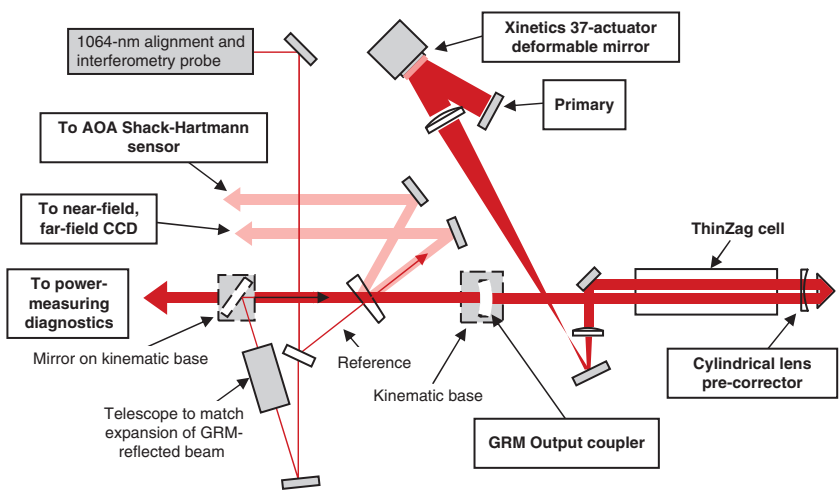

FIGURE 9.11 Folded cavity with increased gain length set up with unstable optics for beam quality measurements. AOA: adaptive optics associates; CCD: charge-coupled device; GRM: graded reflectivity mirror.

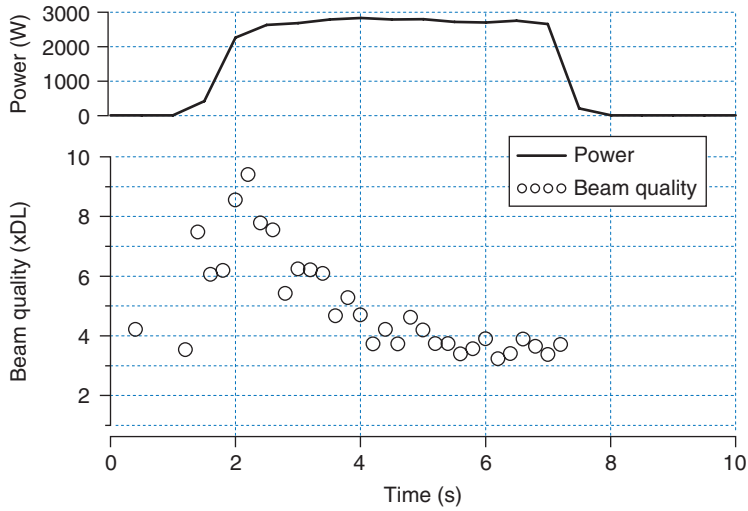

Figure 9.12 Measured beam quality (power in a 1 xDL bucket method) is plotted as a function of time for the TZ-2 cell operation at 3-kW output power.

reduced to about 3 kW, which is substantially below that measured using a stable optical cavity; this reduction was due mainly to the nonoptimum output coupling.

Beam quality measurements for the configuration of Fig. 9.11 are shown in Fig. 9.12, in which beam quality was measured using a CCD camera. The power into the central 1 times diffraction limited (xDL) spot (dimensions determined by the 1×1 cm near-field profile) was measured. The laser was set up using intracavity "precorrector" cylindrical lenses. The beam quality was initially poor, due in part to the medium itself and in part to the distortions caused by the precorrector lenses. An adaptive optics associates (AOA) WaveScope was used to measure the medium phase, and a Xinetics 37-actuator deformable mirror was used to correct the medium. These data show that good beam quality (~3 to 4 xDL) was achieved. At somewhat lower power, beam quality of about 2 xDL was measured. As mentioned earlier, the major distortions established themselves in about a second; however, the beam quality shown in Fig. 9.12 took longer to get to its steady-state value due to software and hardware bandwidth limits of the adaptive optics system used in these preliminary trials. With planned improvements, the AO system's bandwidth is expected to improve by about an order of magnitude.

9.1.3 TZ-3 Module Development

As described earlier, the TZ-3 and TZ-2 lasers have the same footprint and flow manifolds. The key difference between the two devices is

Nd:YAG Ceramic ThinZag® High-Power Laser Development

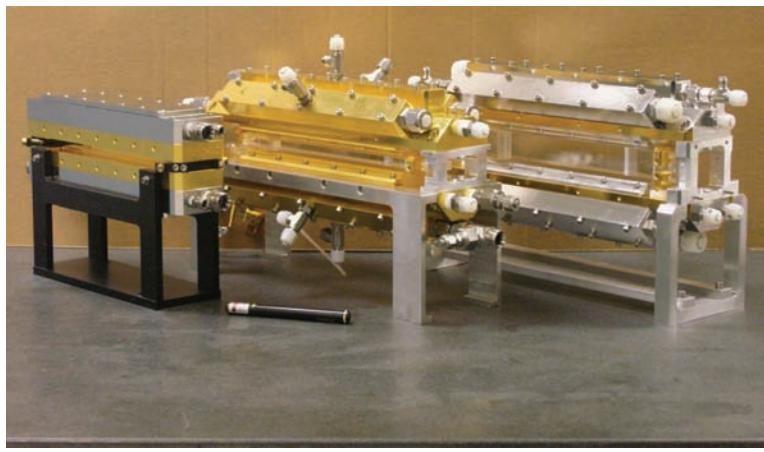

Figure 9.13 The three ThinZag modules: TZ-1, TZ-2, and TZ-3 (from left to right). Interestingly, there is not a significant size change in the modules as the power increases from about 1 kW laser output (TZ-1) to more than 15 kW laser output (TZ-3).

the height of the Nd:YAG slabs. The TZ-2 device uses 1-cm-high slabs, while the TZ-3 uses 3-cm-high slabs. Because the pump intensity in both devices is the same, the output from the TZ-3 module, compared with the TZ-2 module, is expected to be greater by a factor of 3. Since the TZ-2 module produced about 5.6 kW, the TZ-3 is expected to produce about 16.8 kW. Figure 9.13 shows the TZ-1, TZ-2, and TZ-3 lasers. Note the small change in the devices' overall dimensions, which produces more than an order of magnitude higher power when scaling from the TZ-1 to the TZ-3. Initial short-pulse measurements performed on the TZ-3 demonstrated outputs to 16.8 kW output using a stable cavity, as shown in Fig. 9.14.

The TZ-3 laser module operates, as did all the previous ThinZag laser modules, with laser medium distortions that are low order (mainly cylinder) and slowly varying (time scales of seconds). Modifications to the laser module continue to improve the device's thermal control, which in turn influences the medium quality when under full-power extraction.

9.1.4 Coupling Three TZ-3 Modules

Three TZ-3 modules were coupled in series as a single-aperture power oscillator. (Three is the minimum number of modules needed to operate with an unstable cavity for good beam quality.) The laser model calculations shown in Fig. 9.15 indicate that with three modules, optimum feedback for good extraction occurs at a little over 40 percent reflectivity. For graded reflectivity output couplers, the

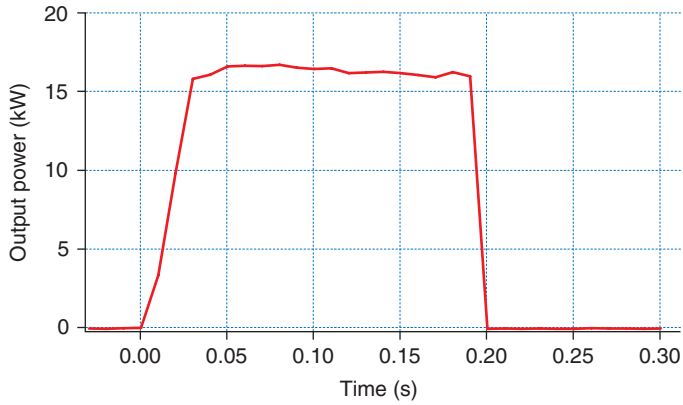

FIGURE 9.14 Short-pulse measurements were made using the TZ-3 module. Output of 16.8 kW was achieved in 200-ms pulses. The calculated optical efficiency (laser output/pump diode output) is 25 percent.

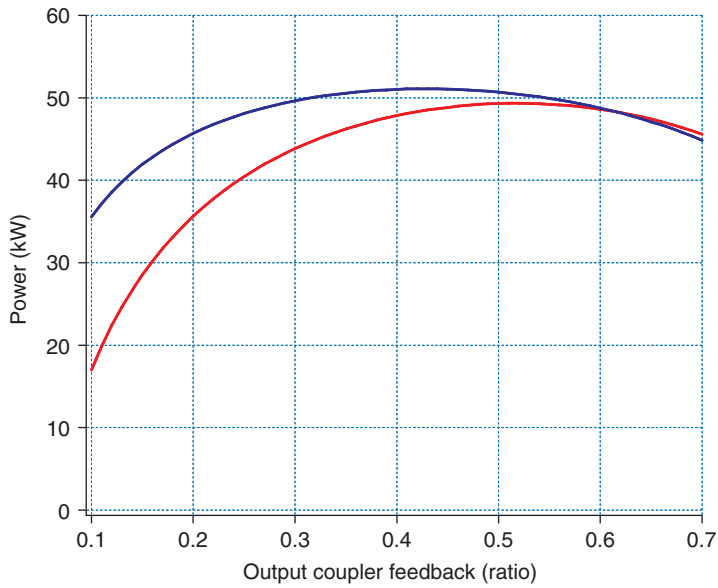

FIGURE 9.15 Model calculations of expected power extraction from three TZ-3 modules. The red curve predicts CW and the blue curve low duty cycle (LDC) performance.

highest feedback that can be achieved is about 40 percent; thus, operating with less than three modules would not allow good extraction. If the laser medium is not operating with good extraction, other loss mechanisms (i.e., amplified spontaneous emission [ASE] or parasitic losses) can further reduce the optical extraction.

The TZ-3 was designed to operate at 100 kW as six modules in a series power oscillator. Each TZ-3 module was designed to be low gain, so that ASE loss along the length of the slab would be minimal when operated at full power. To increase the gain of the modules for more efficient operation, an alternative mode of operation—namely, low duty cycle (LDC)—was tested. In LDC mode, the current is pulsed on for, say, 30 ms and off for 30 ms. The on times and off times are somewhat arbitrary, though the pulse time should be long compared with the kinetic lifetime of Nd:YAG (0.25 ms) and short compared with the slab's thermalization time (~1 s).

During the on time, the current is set much higher than the nominal 80-A full pump current used for CW operation; therefore, the instantaneous gain is much higher. In this case, the laser operates at the maximum allowed current of the Osram diodes. At the higher-diode pump currents, the laser operates at higher gain, with more efficient extraction and consequently lower thermal heating of the slab. The LDC current is chosen such that the laser output essentially doubles for the on time compared with the current for CW operation. For LDC mode, the average laser output is the same as for CW current; however, because of the more efficient extraction, the overall heating of the slabs is reduced, as are thermal distortions. Figure 9.15 shows the calculated improved extraction for lower-output coupling when operating in the LDC mode.

A series of measurements, shown in Fig. 9.16, was performed to test LDC mode operation. Measurements made with stable (S) and unstable (U) optical cavities gave essentially the same average output, as one would expect. The individual 30-ms pulses, measured using a fast-response Labsphere, were twice the average power, as predicted. Kinetic code calculations of the expected output also agreed. The stable optical cavity output power measured was 44 kW, compared with code calculations that predicted 42 kW average power

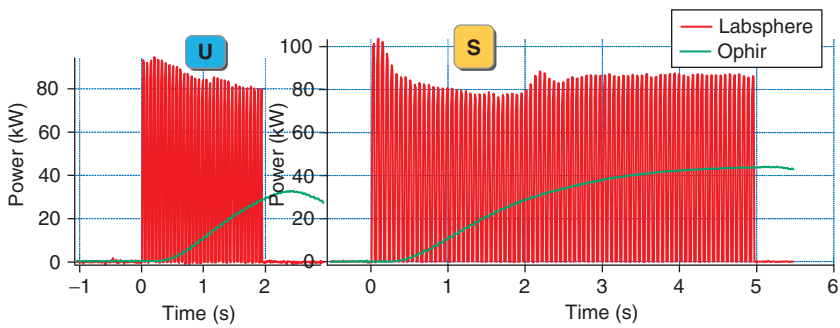

Figure 9.16 Three TZ-3 modules operating with unstable (U) and stable (S) optical cavities. Note that the instantaneous power output is essentially double the average power. Output from stable and unstable cavities is comparable.

for this case. Note that the instantaneous power of the pulses is close to 88 kW, close to calculation.

Several issues must be addressed when using LDC mode. The diode current's rise time must be fast as compared with the several-millisecond pulse on time. The Sorenson SFA-150 power supplies used have current rise times less than 0.25 ms, which is significantly less than the pulse on time. Diode wavelength measurements indicate that the steady-state diode temperature is achieved on the scale of the pulse rise time. A key issue that is yet to be addressed is optimized control of the deformable mirrors in pulsed mode for good beam quality. Controlling deformable mirrors is more straightforward in CW than in LDC mode. The downside is that thermal heating of the slabs is greater in CW mode, so the intrinsic medium distortion is greater.

Figure 9.17 shows the three modules set up as a single-aperture power oscillator. The design of the optical cavity has provisions for operation with a deformable mirror coupled to each cell to correct medium distortion. The distortions are sensed using a second color probe laser; a Shack-Hartmann detector measures phase and controls a deformable mirror to correct the phase of each module. Initial measurements were made without the internal deformable mirrors in the optical cavity. An external deformable mirror built by MZA Associates was used to correct beam quality.

A series of measurements was made at diode pump currents of 50, 60, and 70 A. The optical cavity used a GRM output coupler with a nominal magnification of 1.4. The GRM feedback was still

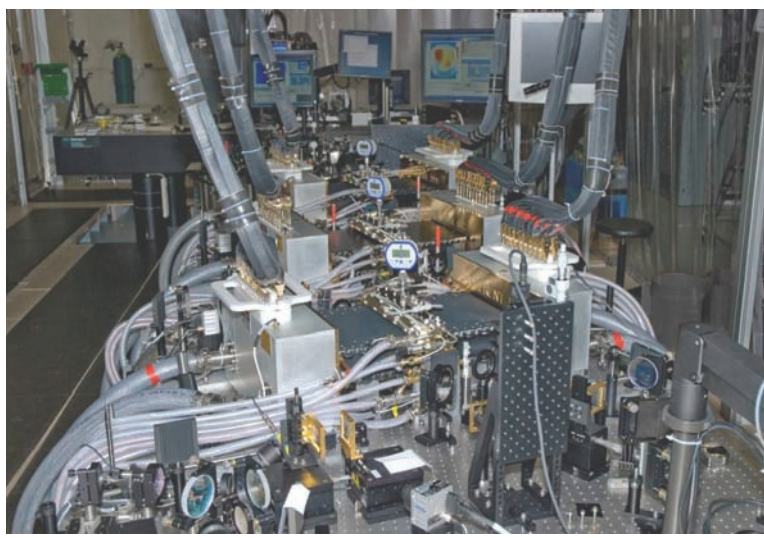

Figure 9.17 Three TZ-3 modules operating as a single-aperture power oscillator.

Nd:YAG Ceramic ThinZag® High-Power Laser Development

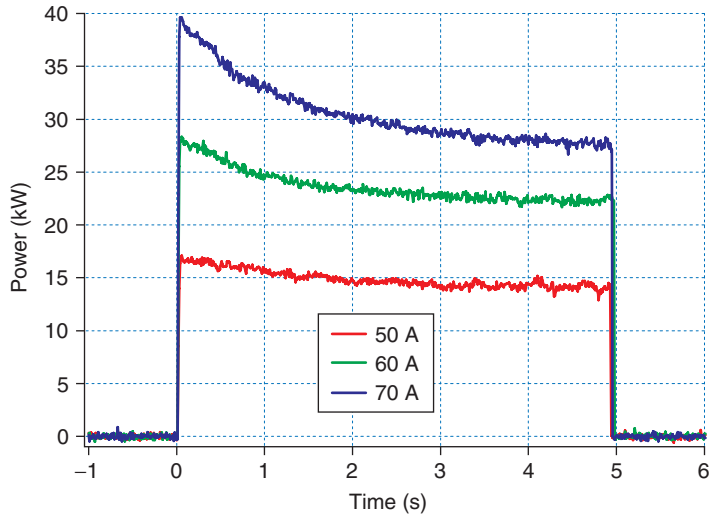

FIGURE 9.18 Characteristic output power from the three-module ThinZag configuration.

somewhat below the optimum feedback needed for the three-module configuration tested.

The laser was operated in 5-s bursts to ensure that steady-state operation was achieved by the end of the run. Characteristic output powers for 5-s runs are shown in Fig. 9.18. Laser output powers of between 15 and 30 kW were achieved with beam qualities of 2.4 xDL at the lower powers and 3.3 xDL at the highest powers. The diode pump source is capable of higher current operation, which should result in increased laser output power.

The next scaling of the device was to couple six TZ-3 modules into a single-aperture laser to produce 100 kW laser output. An engineer's drawing showing six TZ-3 modules on two coupled 5×10 ft optical benches is shown in Fig. 9.19. This device recently achieved

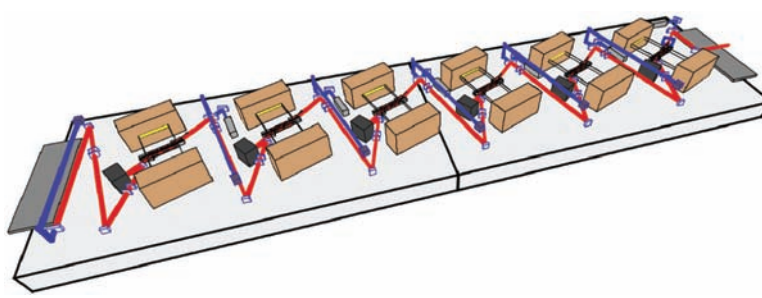

FIGURE 9.19 Layout design for six TZ-3 modules for 100-kW ThinZag laser on two coupled 5×10 ft optical benches.

average powers in excess of 100 kW in final testing on the JHPSSL program.

9.2 Summary

This chapter presented an overview of the approach, history, and current state of scaling Nd:YAG ceramic ThinZag lasers to significant power levels using a single-aperture power oscillator architecture. These lasers are compact and scalable to 100 kW and higher power levels. Recently average power levels in excess of 100-kW output were achieved in final government testing of the JHPSSL program. A critical issue, as with all very high power solid-state lasers, is achieving excellent beam quality at the highest powers.

Acknowledgments

This work was supported by the U.S. Army Space and Missile Defense Technical Center, SMDC-RDTC-TDD, in Huntsville, Alabama, under contract W9113M-05-C-0217, with funding from the Department of Defense (DOD) High Energy Laser Joint Technology Office, in Albuquerque, New Mexico, and from the office of the Secretary of the Army for Acquisition, Logistics, and Technology (ASA-ALT).

The authors wish to acknowledge the excellent technical assistance of R. Hayes for his creative design contributions to the ThinZag device. We also thank R. Budny and M. Trainor, for their invaluable operational support during the course of this research, and M. Foote, for his excellent insights into phase control of this device. We also acknowledge the support of W. Russell and S. Flintoff in the assembly of the ThinZag device. We also thank I. Sadovnik, J. Moran, and C. vonRosenberg for their support on thermal analysis of the laser module.

References

1. Lu, J., Prabhu, M., Song, J., Li, C., Xu, J., Ueda, K., Kaminskii, A. A., Yagi, H., and Yanagitani, T., "Optical Properties and Highly Efficient Laser Oscillation of Nd:YAG Ceramics," *Appl. Phys. B*, 71: 469–473, 2000.
2. Lu, J., Song, J., Prabhu, M., Xu, J., Ueda, K., Yagi, H., Yanagitani, T., and Kudryashov, A., "High Power Nd:$Y_3Al_5O_{12}$ Ceramic Laser," *Jpn. J. Appl. Phys.*, 39: L1048–L1050, 2000.
3. Lu, J., Murai, T., Takaichi, K., Umeatsu, T., Misawa, K., Ueda, K., Yagi, H., Yanagitani, T., and Kaminskii, A. A., "Highly Efficient Polycrystalline Nd:YAG Ceramic Laser," Solid State Lasers X, *Proc. SPIE*, 4267: 2001.
4. Mandl, A., and Klimek, D. E., "Multipulse Operation of a High Average Power, Good Beam Quality Zig-Zag Dye Laser," *IEEE J. Quantum Electron.*, 32: 378–382, 1996.
5. Mandl, A., and Klimek, D. E., "Single Mode Operation of a Zig-Zag Dye Laser," *IEEE J. Quantum Electron.*, 31: 916–922, 1995.
6. Mandl, A., Zavriyev, A., and Klimek, D. E., "Energy Scaling and Beam Quality Improvement of a Zig-Zag Solid-State Plastic Dye Laser," *IEEE J. Quantum Electron.*, 32: 1723–1726, 1996.

7. Mandl, A., Zavriyev, A., Klimek, D. E., and Ewing, J. J., "Cr:LiSAF Thin Slab Zigzag Laser," *IEEE J. Quantum Electron.*, 33: 1864–1868, 1997.
8. Mandl, A., Zavriyev, A., and Klimek, D. E., "Flashlamp Pumped Cr:LiSAF Thin-Slab Zig-Zag Laser," *IEEE J. Quantum Electron.*, 34: 1992–1995, 1998.
9. Klimek, D. E., and Mandl, A., "Power Scaling of Flashlamp-Pumped Cr:LiSAF Thin-Slab Zig-Zag Laser," *IEEE J. Quantum Electron.*, 38: 1607–1613, 2002.
10. Lu, J., Murai, T., Takaichi, K., Umeatsu, T., Misawa, K., Ueda, K., Yagi, H., and Yanagitani, T., "72 W Nd:YAG Ceramic Laser," *Appl. Phys. Lett.*, 78: 3586–3588, 2001.
11. Heller, A. "Transparent Ceramics Spark Laser Advances," Livermore National Research Laboratory Science and Technology Review, *S&TR,* Apr. 2006.